of the rather specific requirements for halide binding both within and between the clusters. For this reason ternary systems have also been under investigation, leading to the discovery of $CsNb_6I_{11}$,[24] the present $CsZr_6I_{14}$ as sort of an intercalate of a known structure type, and, recently, the analogous $NaNb_6Cl_{15}$ with the Nb_6Cl_{15} structure and a new structure type for $CsNb_6Cl_{15}$.[30] Obviously the use of a higher-valent second metal, especially with the electron-poorer clusters, seems attractive, for example, with MZr_6I_{14}, where M = Ba would give a cluster isoelectronic with Zr_6I_{12}. Doubtlessly, less obvious derivatives will be found as well.

(30) Imoto, H.; Simon, A., private communication, 1981.

Acknowledgment. The authors are indebted to R. A. Jacobson for continued crystallographic advice, to R. G. Barnes and D. T. Torgeson for assistance in ESR measurements, and to D. M. P. Mingos and P. Minshall for assistance in the computation, time for which was provided by the Inorganic Chemistry Laboratory, Oxford University.

Registry No. Zr_6I_{12}, 66908-75-6; $CsZr_6I_{14}$, 82456-16-4; ZrI_4, 13986-26-0; Zr, 7440-67-7; CsI, 7789-17-5.

Supplementary Material Available: A listing of structure factor amplitudes for Zr_6I_{12} and $CsZr_6I_{14}$ (6 pages). Ordering information is given on any current masthead page.

Contribution from the Department of Chemistry and Materials Research Laboratory, University of Illinois, Urbana, Illinois 61801, and the Department of Chemistry, State University of New York at Buffalo, Buffalo, New York 14214

Vibrational Study and Crystal Structure of (μ-Hydrido)(μ-formato)decacarbonyltriosmium, (μ-H)(μ-O_2CH)$Os_3(CO)_{10}$[1]

JOHN R. SHAPLEY,*[2] GEORGE M. ST. GEORGE,[2] MELVYN ROWEN CHURCHILL,*[3] and FREDERICK J. HOLLANDER[3]

Received December 16, 1981

The formate compounds (μ-H)(μ-$O_2{}^{12}$CH)$Os_3(CO)_{10}$, (μ-H)(μ-O_2CD)$Os_3(CO)_{10}$, and (μ-H)(μ-$O_2{}^{13}$CH)$Os_3(CO)_{10}$ have been prepared from the reactions of $Os_3(CO)_{10}(C_8H_{14})_2$ with the acids $H^{12}CO_2H$, DCO_2H, and $H^{13}CO_2H$, respectively. Infrared data on the formate ligand vibrational modes in these compounds were collected and assigned. The assignments were supported by an approximate normal-coordinate analysis of the vibrationally isolated formate group. The carbon–hydrogen stretching frequency is unusually high for a formate complex, which is interpreted to indicate considerable charge transfer to the $Os_3(CO)_{10}$ unit. Comparison of the formate frequencies found for the molecular complexes (μ-H)(μ-O_2CH)$Os_3(CO)_{10}$ and (μ-H)(μ-O_2CD)$Os_3(CO)_{10}$ with those observed for chemisorbed HCO_2^- and DCO_2^- on Ag(110) by Sexton and Madix shows good overall correspondence. The complex (μ-H)(μ-O_2CH)$Os_3(CO)_{10}$ crystallizes in the triclinic space group $P\bar{1}$ with a = 7.9683 (15) Å, b = 15.316 (2) Å, c = 15.744 (2) Å, α = 65.834 (11)°, β = 80.100 (13)°, γ = 88.184 (14)°, V = 1725.4 (5) Å^3, and Z = 4 (i.e., *two* molecules per asymmetric unit). Diffraction data (Mo Kα, 2θ = 445°) were collected with a Syntex $P2_1$ automated four-circle diffractometer, and the structure was solved by conventional methods. All nonhydrogen atoms were located, and final discrepancy indices were R_F = 4.75% and R_{wF} = 3.25% for the 4538 unique reflections. Each independent molecule in the unit cell contains a triangular triosmium core in which one osmium atom (Os(3)) is linked to four terminal carbonyl ligands; the other two osmium atoms (Os(1) and Os(2)) are each linked to three terminal carbonyl ligands, are bridged diaxially by a formate moiety, and are bridged diequatorially by a hydride ligand (which was *not* located directly but which had an apparent position). Each molecule possesses approximate C_s symmetry. The Os_3 plane makes an obtuse angle (average 98.6°) with the O(1)–Os(1)–Os(2)–O(2) "coordination plane"; the formate ligand (defined by O(1)–C(1)–O(2)) bends outward by a further small amount (average 5.3°). The bridged osmium–osmium distances (average Os(1)–Os(2) 2.908 Å) are 0.033 Å larger than the nonbridged intermetallic distances (average 2.875 Å).

Introduction

The metal-catalyzed decomposition of formic acid has been studied extensively, and chemisorbed formate is implicated as an intermediate.[4] Infrared spectroscopy, either in the transmission mode for supported metals[5] or in the reflectance mode for metal films,[6] has been used to observe surface formate species. Recently, however, electron energy loss spectroscopy has been applied to the study of formate species formed on Cu(100)[7] and Ag(110)[8] crystal surface planes. Comparison of vibrational data represents one of the few means of examining a particular moiety both as a chemisorbate on a metal surface and as a ligand in a structurally well-characterized molecular metal complex.[9] Since the title compound[10] contains only carbonyl ligands in addition to the elements of formic acid, it appeared to be an especially suitable model compound. We have prepared isotopically labeled versions of the compound and have obtained and analyzed infrared data on the formate ligand in order to allow a comparison with vibrational data on surface formate species.

From a purely structural point of view, we have examined a number of (μ-H)(μ-L)$O_3(CO)_{10}$ compounds of type I, in which the bridging hydride ligand and the ligand L occupy sites intermediate between axial and equatorial. These include (μ-H)$_2Os_3(CO)_{10}$,[11] (μ-H)(μ-CHCH$_2$PMe$_2$Ph)$Os_3(CO)_{10}$,[15]

(1) This paper is considered to be part 23 in the series "Structural Studies on Polynuclear Osmium Carbonyl Hydrides". For previous parts see: (a) Part 20: Churchill, M. R.; Bueno, C.; Kennedy, S.; Bricker, J. C.; Plotkin, J. S.; Shore, S. G. *Inorg. Chem.* **1982**, *21*, 627. (b) Part 21: Shapley, J. R.; Samkoff, D. E.; Bueno, C.; Churchill, M. R. *Ibid.* **1982**, *21*, 634. (c) Part 22: Churchill, M. R.; Bueno, C.; Hsu, W. L.; Plotkin, J. S.; Shore, S. G. *Ibid.* **1982**, *21*, 1958.
(2) University of Illinois.
(3) State University of New York at Buffalo.
(4) For a recent review see: Madix, R. J. *Adv. Catal.* **1980**, *29*, 1.
(5) Little, L. H. "Infrared Spectra of Adsorbed Species"; Academic Press: New York, 1966.
(6) Ito, M.; Suetaka, W. *J. Catal.* **1978**, *54*, 13 and references therein.
(7) Sexton, B. A. *Surf. Sci.* **1979**, *88*, 319.
(8) Sexton, B. A.; Madix, R. J. *Surf. Sci.* **1981**, *105*, 177.
(9) For a recent review, see: Muetterties, E. L.; Rhodin, T. N.; Band, E.; Brucker, C. F.; Pretzer, W. R. *Chem. Rev.* **1979**, *79*, 91.
(10) Bryan, E. G.; Johnson, B. F. G.; Lewis, J. *J. Chem. Soc., Dalton Trans.* **1977**, 1328.
(11) Part 5: Churchill, M. R.; Hollander, F. J.; Hutchinson, J. P. *Inorg. Chem.* **1977**, *16*, 2697. See also ref 12–14.

0020-1669/82/1321-3295$01.25/0

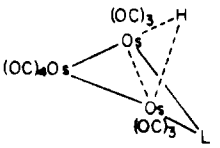

I

$(\mu\text{-H})(\mu\text{-CHCH=NEt}_2)\text{Os}_3(\text{CO})_{10}$,[16] $(\mu\text{-H})(\mu\text{-Cl})\text{Os}_3(\text{CO})_{10}$,[17a] $(\mu\text{-H})(\mu\text{-Br})\text{Os}_3(\text{CO})_{10}$,[17b] $(\mu\text{-H})(\mu\text{-OMe})\text{Os}_3(\text{CO})_{10}$,[18] and $(\mu\text{-H})(\mu\text{-NHSO}_2\text{C}_6\text{H}_4\text{Me})\text{Os}_3(\text{CO})_{10}$.[19]

Compounds of the formula $(\mu\text{-H})(\mu\text{-L})\text{Os}_3(\text{CO})_{10}$, in which L is a diaxially bridging ligand and the hydride ligand is truly equatorial, are less well characterized.[1b,20-22] The species $(\mu\text{-H})(\mu\text{-O}_2\text{CH})\text{Os}_3(\text{CO})_{10}$, examined herein, is shown to be of this type (see II).

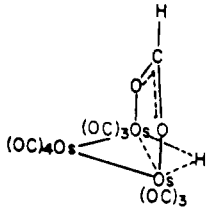

II

Experimental Section

Preparation of Compounds. Solvents and readily available reactants were reagent grade and generally were used without further purification. Preparative thin-layer chromatography was conducted with Merck silica gel G (type 60). $\text{Os}_3(\text{CO})_{12}$[23] and $\text{H}_2\text{Os}_3(\text{CO})_{10}$[24] were prepared by published procedures. $\text{Os}_3(\text{CO})_{10}(\text{C}_8\text{H}_{14})_2$[25] was used as a cyclooctene solution of concentration 0.03 mmol/mL. ^{1}H NMR spectra were recorded on a Varian EM-390 spectrometer at 90 MHz. ^{13}C NMR spectra were recorded on a Varian XL-100 spectrometer at 25 MHz. Elemental analyses were performed at the University of Illinois by the microanalytical laboratory of the School of Chemical Sciences.

$(\mu\text{-H})(\mu\text{-O}_2\text{CH})\text{Os}_3(\text{CO})_{10}$. To 4.0 mL of the cyclooctene solution of $\text{Os}_3(\text{CO})_{10}(\text{C}_8\text{H}_{14})_2$ (0.12 mmol) was added 5 mL of formic acid, and the mixture was magnetically stirred for 30 min under N_2. Formic acid and cyclooctene were removed in vacuo, and the residue was purified by thin-layer chromatography. The desired product appeared as the predominant yellow band. Yellow crystals were obtained from chloroform, carbon tetrachloride, or carbon disulfide solutions by evaporation or by adding ethanol to a saturated carbon tetrachloride solution and cooling to −15 °C; yield 65 mg, 0.073 mmol, 61%. Anal. Calcd for $\text{C}_{11}\text{H}_2\text{O}_{12}\text{Os}_3$: C, 14.73; H, 0.22; Os, 63.63. Found: C, 15.09; H, 0.24; Os, 63.2. ^{1}H NMR (CCl_4, 30 °C): δ 7.4 (s, 1 H), −10.5 (s, 1 H), consistent with literature values.[10] IR (CCl_4): ν_{CO} 2115 (m), 2076 (vs), 2064 (vs), 2028 (vs), 2015 (vs), 1996 (s), 1991 (s), 1974 (vw), 1961 (vs) cm^{-1}.

$(\mu\text{-H})(\mu\text{-O}_2\text{CD})\text{Os}_3(\text{CO})_{10}$. DCO_2H was prepared by a modification of the method of Sprinson.[26] Potassium cyanide (1.5 g, 0.024 mol), water-d_2 (99.5% D, 2.0 mL, 0.11 mol), and sodium hydroxide (0.05 g, 1.25 mmol) were sealed in a thick-walled glass tube (volume 100 mL) and heated at 170 °C for 5 h. After cooling, the tube was opened, and the resulting ammonia was released. The remaining mixture was acidified with concentrated sulfuric acid and extracted with diethyl ether. The ether was distilled off, leaving ca. 1 mL of DCO_2H. To this were added water (2 mL) and $\text{Os}_3(\text{CO})_{10}(\text{C}_8\text{H}_{14})_2$ solution (4.0 mL, 0.12 mmol). The reaction and subsequent workup were the same as described above: yield 58 mg, 0.065 mmol, 54%; ^{1}H NMR (CCl_4, 30 °C) δ −10.5 (s, 1 H).

$(\mu\text{-H})(\mu\text{-O}_2{}^{13}\text{CH})\text{Os}_3(\text{CO})_{10}$. $\text{H}^{13}\text{CO}_2\text{H}$ was prepared by a modification of the method of Geuther.[27] Sodium hydroxide (4.0 g, 0.10 mol) was finely ground, oven-dried, and placed in a 300-mL pressure bottle.[28] The vessel was evacuated, pressurized to 18 psig with ^{13}CO (90% ^{13}C enriched, Mound Laboratories), and heated to 170 °C for 6 h. After the vessel cooled, residual CO was released, the solid residue reground to provide fresh surface area, and the pressurization repeated. The solid was dissolved in the minimum amount of water and filtered to remove carbon black, and the solution was acidified with concentrated sulfuric acid and distilled to give ca. 3 mL of aqueous $\text{H}^{13}\text{CO}_2\text{H}$. This was added to the $\text{Os}_3(\text{CO})_{10}(\text{C}_8\text{H}_{14})_2$ solution (8.0 mL, 0.25 mmol), and the product was purified as above: yield 137 mg, 0.154 mmol, 64%; ^{1}H NMR (CCl_4, 30 °C) δ 7.4 (d, 1 H, $^1J_{CH}$ = 219 Hz), −10.5 (s, 1 H); ^{13}C NMR (CDCl_3, 30 °C) δ 179.1 (d, 1 C, $^1J_{CH}$ = 219 Hz).

Collection of X-ray Diffraction Data. Crystals of $(\mu\text{-H})(\mu\text{-O}_2\text{CH})\text{Os}_3(\text{CO})_{10}$ are clear yellow with a natural "bladelike" habit and tend to aggregate into clusters. Several crystals were taken from one such aggregate, trimmed to suitable dimensions and mounted on glass fibers in air with GE Varnish. These were then examined optically and examined by means of precession photographs. The best crystal (on the basis of spot intensity vs. size) was brick-shaped

Table I. Data for the X-ray Diffraction Study of $(\mu\text{-H})(\mu\text{-O}_2\text{CH})\text{Os}_3(\text{CO})_{10}$

A. Crystal Data at 24 °C

cryst syst: triclinic	V = 1725.4 (5) Å^3
space group: $P\bar{1}$	Z = 4 (i.e., *two* molecules per asym unit)
a = 7.9683 (15) Å	mol wt = 896.7
b = 15.316 (2) Å	ρ(calcd) = 3.45 g/cm^3
c = 15.744 (2) Å	μ(calcd) = 221 cm^{-1}
α = 65.834 (11)°	
β = 80.100 (13)°	
γ = 88.184 (14)°	

B. Measurement of Intensity Data

diffractometer: Syntex $P2_1$
radiation: Mo Kα ($\bar{\lambda}$ = 0.710 730 Å)
monochromator: pyrolytic graphite (equatorial)
reflctns measd: $+h, \pm k, \pm l$; $4.0° < 2\theta < 45°$
scan type: coupled θ(cryst)-2θ(counter)
scan range: sym, $[1.8° + \Delta(\alpha_2 - \alpha_1)]°$
bkgd: stationary cryst and counter, at each end of scan range, for each for $^1/_4$ time of scan
scan speed: 3.0°/min
reflctns collected: 4931 total, reduced to 4538 unique reflctns
std reflctns: intensities of the 500, 0,10,2, and 328 reflctns measd after every 75 data points

C. Data for Absorption Corrections

h	k	l	2θ, deg	I_{max}/I_{min}
2	0	4	14.11	1.94
2	1	6	17.74	2.06
3	2	8	24.21	1.90
4	1	9	29.71	1.64
5	2	10	34.38	1.54

(12) Allen, V. F.; Mason, R.; Hitchcock, P. B. *J. Organomet. Chem.* **1977**, *140*, 297.
(13) Orpen, A. G.; Rivera, A. V.; Bryan, E. G.; Pippard, D.; Sheldrick, G. M.; Rouse, K. D. *J. Chem. Soc., Chem. Commun.* **1978**, 723.
(14) Broach, R. W.; Williams, J. M. *Inorg. Chem.* **1979**, *18*, 314.
(15) Part 2: Churchill, M. R.; DeBoer, B. G. *Inorg. Chem.* **1977**, *16*, 1141.
(16) Part 11: Churchill, M. R.; Lashewycz, R. A. *Inorg. Chem.* **1979**, *18*, 848.
(17) (a) Part 12: Churchill, M. R.; Lashewycz, R. A. *Inorg. Chem.* **1979**, *18*, 1926. (b) Part 13: Churchill, M. R.; Lashewycz, R. A. *Ibid.* **1979**, *18*, 3261.
(18) Part 16: Churchill, M. R.; Wasserman, H. J. *Inorg. Chem.* **1980**, *19*, 2391.
(19) Part 15: Churchill, M. R.; Hollander, F. J.; Shapley, J. R.; Keister, J. B. *Inorg. Chem.* **1980**, *19*, 1272.
(20) Guy, J. J.; Sheldrick, G. M. *Acta Crystallogr., Sect. B* **1978**, *B34*, 1718.
(21) (a) Adams, R. D.; Golembeski, N. M. *Inorg. Chem.* **1978**, *17*, 1969. (b) Adams, R. D.; Golembeski, N. M. *J. Am. Chem. Soc.* **1979**, *101*, 2579.
(22) (a) Adams, R. D.; Selegue, J. P. *J. Organomet. Chem.* **1980**, *195*, 223. (b) Adams, R. D.; Golembeski, N. M.; Selegue, J. P. *J. Am. Chem. Soc.* **1981**, *103*, 546.
(23) Bradford, C. W.; Nyholm, R. S. *Chem. Commun.* **1967**, 384.
(24) Knox, S. A. R.; Koepke, J. W.; Andrews, M. A.; Kaesz, H. D. *J. Am. Chem. Soc.* **1975**, *97*, 3942.
(25) Tachikawa, M.; Shapley, J. R. *J. Organomet. Chem.* **1977**, *124*, C19.
(26) Elwyn, D.; Weissback, A.; Henry, S. S.; Sprinson, D. B. *J. Biol. Chem.* **1955**, *213*, 281.
(27) Geuther, A. *Justus Liebigs Ann. Chem.* **1880**, *202*, 288.
(28) Barefield, E. K. *J. Chem. Educ.* **1973**, *50*, 689.

with approximate dimensions at 0.11 mm × 0.15 mm × 0.15 mm. It was used for all further crystallographic work on the compound. This crystal was transferred to our Syntex $P2_1$ four-circle diffractometer and accurately centered. Determinations of preliminary unit cell parameters and orientation matrix were carried out as previously described.[29]

Our preliminary studies had indicated no crystallographic symmetry (other than the Friedel conditions) for the crystal, and this judgement was verified by a cell reduction procedure on the unit cell parameters found.

Accurate cell parameters were determined by least-squares refinement on the setting angles of 12 Friedel pairs of reflections well separated in reciprocal space and having 2θ values between 22 and 30° (Table I).

Inspection of data taken for certain close-to-axial reflections at 10° intervals at rotation of the crystal about the diffraction vector (ψ) showed a variation of intensity of I_{max}/I_{min} smaller than 2/1 in all cases. This was judged acceptable, and data collection proceeded as described previously.[29] Details are given in Table I.

Data were reduced to net intensities (I) and esd's ($\sigma(I)$) as shown in eq 1 and 2, where CT, B_1, and B_2 are the counts associated with

$$I = \mathrm{CT} - \tau(B_1 + B_2) \quad (1)$$

$$\sigma(I) = [\mathrm{CT} + \tau^2(B_1 + B_2)]^{1/2} \quad (2)$$

the scan and the first background and second background measurements, respectively, and τ (=2 in the present case) is the ratio of time taken for the scan to the total time taken in measuring the background. The data were then corrected for absorption by the empirical method described previously (see Table I, section C, and ref 30).

All of the curves of relative intensity vs. ϕ were of the same general shape and had maxima and minima at the same values of ϕ.

The 4931 data were then averaged according to $\bar{1}$ symmetry to give 4538 unique reflections. The R factor for agreement in I, $R_{av}(I)$ (see eq 3), was 2.26% for the 392 symmetry-related pairs of reflections.

$$R_{av}(I) = [(\Sigma||I| - |I_{av}||)/\Sigma|I|] \times 100 \quad (3)$$

For these reflections the esd of the intensity was taken as the larger of that calculated from counting statistics and that calculated by deviation from the mean.

Intensities were finally converted to (unscaled) observed structure factor amplitudes after application of Lorentz and polarization factors (monochromator in equatorial mode, assumed to be 50% perfect). Esd's of the F_o values were calculated by finite differences from $\sigma_o(F^2)$. F_o was set to 0.0 if the net intensity of the reflection was ≤ 0.0.

Solution and Refinement of the Structure. Data reduction and calculation of the Patterson map were performed with use of our in-house Syntex XTL structure determination package.[31] The data were then transferred via magnetic tape to the CDC 6600/Cyber 173 computer system at SUNY—Buffalo, where all further calculations were performed. Programs used include DATRE (data transfer from IBM- to CDC-compatible format), JIMDAP (Fourier synthesis, derived from A. Zalkin's FORDAP, by J. A. Ibers and co-workers), LSHF (full-matrix least-squares refinement, by B. G. DeBoer), STAN1 (distances and angles, with esd's, by B. G. DeBoer), PLOD (least-squares planes, by B. G. DeBoer), and ORTEP-II (thermal ellipsoid plots, by C. K. Johnson).

The analytical scattering factors compiled by Cromer and Waber[32a] were used throughout the analysis and were corrected for both the real ($\Delta f'$) and the imaginary ($\Delta f''$) components of anomalous dispersion[32b] for all nonhydrogen atoms.

The function minimized during least-squares refinement was $\sum w(|F_o| - |F_c|)^2$, where the "ignorance factor" (p) was given a value of 0.02 and the expression for the weight (w) is given by eq 4.

$$w = [\sigma_o^2(|F_o|) + (0.02|F_o|^2)^2]^{-1} \quad (4)$$

The three-dimensional Patterson map was solved to give the positions of the osmium atoms of the *two* molecules that define the asymmetric unit of the cell. Full-matrix least-squares refinement (with isotropic thermal parameters) followed by a difference-Fourier synthesis revealed all remaining nonhydrogen atoms in the cell.

Due to space limitations in the computer, refinement was continued in blocks—at first consisting of the two independent molecules and later (as all atoms were allowed to refine with anisotropic thermal parameters) in three blocks. These consisted of (i) Os(1A), Os(2A), and their ligands, (ii) similar atoms for molecule B, and (iii) Os(3A), Os(3B), and their ligands. The scale factor was varied as one of the parameters in each blocked cycle. During the last few cycles of a least-squares refinement an isotropic secondary extinction parameter (c) was included. This enters the equation for the corrected calculated structure factor as shown in eq 5; β is defined in eq 6 (cf. ref 33–35). The final value of c was 1.33×10^{-8} e^{-2}.

$$F_{c,cor} = F_{c,uncor}(1 + c\beta F_{c,uncor}^2)^{-1/4} \quad (5)$$

$$\beta = \frac{1 + \cos^4 2\theta}{(\sin 2\theta)(1 + \cos^2 2\theta)} \quad (6)$$

Following convergence, a final cycle of refinement was run in which all positional parameters were varied; this provided the full correlation matrix for use in STAN1.

The final discrepancy indices were $R_F = 4.16\%$, $R_{wF} = 3.18\%$, and GOF = 1.406 for those 4291 data with $|F_o| > 0$; the residuals for all 4538 data were $R_F = 4.75\%$ and $R_{wF} = 3.25\%$. All shifts in the last cycle of refinement for the parameter under consideration were essentially zero ($(\Delta/\sigma)_{max} < 0.03$).

A final difference-Fourier synthesis showed no unexpected features; various attempts to locate directly the hydride ligands or the formate hydrogens were unsuccessful.

Final positional and thermal parameters are collected in Tables II and III.

Vibrational Studies. For most of this work the infrared spectra were recorded with Perkin-Elmer 599B and 281B spectrophotometers on concentrated solutions in Spectrograde solvents (CCl_4, 3500–1300 cm^{-1}; CS_2, 1300–400 cm^{-1}). The spectra of (μ-H)(μ-O_2CH)$Os_3(CO)_{10}$ and (μ-H)(μ-O_2CD)-$Os_3(CO)_{10}$ were obtained also in KBr pellets with a Nicolet 7199C FT-IR spectrometer.

The vibrational analysis was approximate in that only the six internal modes of the formate ligand were considered. The **G** and **F** matrices were calculated with the aid of computer programs written by Schachtschneider as modified by Purcell.[36] The equilibrium coordinates of the atoms were assumed to be the averages of the positions found in the crystal structure. The hydrogen (deuterium) atom was assumed to be on the C_2 axis bisecting the O–C–O bond angle, giving the ligand C_{2v} symmetry. Symmetry coordinates for the ligand are given in Table IV. Force constants were calculated by iterative fitting to the 16 observed frequencies. However, even this number of input frequencies did not uniquely determine the force field. A variety of initial choices for the force constants involving the antisymmetric coordinates (S_4–S_6) were

(29) Churchill, M. R.; Lashewycz, R. A.; Rotella, F. J. *Inorg. Chem.* **1977**, *16*, 265.
(30) Churchill, M. R.; Hollander, F. J.; Hutchinson, J. P. *Inorg. Chem.* **1977**, *16*, 2655.
(31) "Syntex XTL Operation Manual", 2nd ed.; Syntex Analytical Instruments (now Nicolet XRD Division): Cupertino, CA, 1976.
(32) "International Tables for X-ray Crystallography"; Kynoch Press: Birmingham, England, 1974; Vol. 4: (a) pp 99–101; (b) pp 149–150.
(33) Zachariasen, W. H. *Acta Crystallogr.* **1963**, *16*, 1139.
(34) Zachariasen, W. H. *Acta Crystallogr.* **1967**, *23*, 588.
(35) Larson, A. C. In "Crystallographic Computing"; Ahmed, F. R., Ed.; Munksgaard: Copenhagen, 1970; p 29 ff.
(36) Purcell, K. F. Ph.D. Thesis, University of Illinois, Urbana, IL, 1965.

Table II. Positional Parameters for $(\mu\text{-H})(\mu\text{-O}_2\text{CH})\text{Os}_3(\text{CO})_{10}$

atom	x	y	z
	(a) Molecule A		
Os(1A)	0.03418 (7)	0.02286 (4)	0.32072 (4)
Os(2A)	0.29017 (8)	0.14719 (4)	0.16501 (4)
Os(3A)	0.29727 (7)	−0.05730 (4)	0.22896 (4)
O(1A)	0.2009 (12)	0.0542 (6)	0.4003 (6)
O(2A)	0.4008 (13)	0.1456 (7)	0.2815 (7)
C(1A)	0.3332 (20)	0.1066 (10)	0.3666 (11)
O(11A)	−0.2507 (16)	0.1171 (8)	0.4068 (8)
O(12A)	−0.0393 (17)	−0.1794 (8)	0.4744 (9)
O(13A)	−0.2048 (15)	−0.0065 (10)	0.2065 (9)
O(21A)	0.2572 (19)	0.3613 (8)	0.1063 (9)
O(22A)	0.6470 (16)	0.1646 (9)	0.0503 (8)
O(23A)	0.1183 (16)	0.1654 (8)	0.0018 (8)
O(31A)	0.6077 (15)	−0.0607 (9)	0.0871 (9)
O(32A)	0.2066 (18)	−0.2724 (9)	0.3314 (9)
O(33A)	0.0771 (17)	−0.0562 (9)	0.0861 (9)
O(34A)	0.5027 (15)	−0.0655 (8)	0.3808 (8)
C(11A)	−0.1414 (20)	0.0847 (11)	0.3746 (11)
C(12A)	−0.0167 (19)	−0.1054 (11)	0.4171 (10)
C(13A)	−0.1126 (21)	0.0033 (10)	0.2473 (11)
C(21A)	0.2603 (22)	0.2818 (12)	0.1330 (12)
C(22A)	0.5212 (23)	0.1558 (11)	0.0939 (11)
C(23A)	0.1820 (22)	0.1567 (11)	0.0621 (12)
C(31A)	0.4936 (21)	−0.0598 (10)	0.1409 (11)
C(32A)	0.2349 (19)	−0.1943 (13)	0.2964 (12)
C(33A)	0.1523 (21)	−0.0519 (11)	0.1359 (12)
C(34A)	0.4271 (19)	−0.0591 (10)	0.3239 (11)
	(b) Molecule B		
Os(1B)	−0.30929 (7)	0.60774 (4)	0.27988 (4)
Os(2B)	−0.11797 (7)	0.43552 (4)	0.34728 (4)
Os(3B)	−0.31841 (8)	0.46793 (4)	0.20207 (4)
O(1B)	−0.0619 (13)	0.6656 (7)	0.1939 (7)
O(2B)	0.0885 (11)	0.5334 (7)	0.2489 (7)
C(1B)	0.0682 (22)	0.6213 (11)	0.2000 (11)
O(11B)	−0.2700 (16)	0.7632 (8)	0.3518 (9)
O(12B)	−0.4998 (18)	0.7331 (9)	0.1233 (9)
O(13B)	−0.6337 (15)	0.5285 (8)	0.4155 (9)
C(21B)	0.0678 (14)	0.3972 (7)	0.5139 (8)
C(22B)	0.0527 (15)	0.2763 (8)	0.3051 (9)
O(23B)	−0.3924 (17)	0.2966 (9)	0.4923 (8)
O(31B)	−0.2368 (21)	0.2880 (10)	0.1660 (12)
O(32B)	−0.5615 (16)	0.5636 (9)	0.0624 (8)
O(33B)	−0.6323 (17)	0.3620 (9)	0.3532 (9)
O(34B)	−0.0058 (17)	0.5725 (9)	0.0542 (9)
C(11B)	−0.2819 (18)	0.7049 (10)	0.3274 (10)
C(12B)	−0.4258 (21)	0.6850 (11)	0.1807 (11)
C(13B)	−0.5165 (20)	0.5595 (11)	0.3619 (11)
C(21B)	0.0071 (19)	0.4148 (9)	0.4506 (11)
C(22B)	−0.0114 (20)	0.3355 (11)	0.3217 (11)
C(23B)	−0.2940 (23)	0.3488 (12)	0.4363 (13)
C(31B)	−0.2703 (24)	0.3502 (13)	0.1856 (12)
C(32B)	−0.4696 (22)	0.5312 (11)	0.1120 (10)
C(33B)	−0.5171 (21)	0.4027 (11)	0.2995 (11)
C(34B)	−0.1135 (22)	0.5351 (12)	0.1100 (11)

refined to essentially the same values in all cases, but two significantly different sets of refined force constants fit the frequencies involving the symmetric coordinates (S_1–S_3) with almost identical precision (average error 3–4 cm^{-1}). The major differences between the two force fields were in the values of F_{22}, the stretching force constant for $\nu^s_{CO_2}$, and F_{23}, the interaction constant between $\nu^s_{CO_2}$ and δ_{OCO}. In the one case F_{22} (8.219 mdyn/Å) was comparable with F_{44} (for $\nu^a_{CO_2}$) and F_{23} was small and negative (−0.188 mdyn/Å). In the other case F_{22} (13.754 mdyn/Å) was significantly greater than F_{44} and F_{23} was relatively large and positive (1.652 mdyn/Å). Test calculations on sodium formate showed an analogous situation.[37] In the published normal-coordinate analysis of sodium formate,[38] the second type of force field was presented. On the basis of orbital following arguments,[39] the interaction constant between $\nu^s_{CO_2}$ and δ_{OCO} is expected to be positive (i.e., stretching both C–O bonds makes opening the OCO angle more difficult and vice versa), and therefore we also have adopted the second case. The complete set of refined force constants is displayed in Table V. These best values were determined for r_{CH} = 1.05 Å (also r_{CO} = 1.25 Å), although the calculations were relatively insensitive to this parameter.

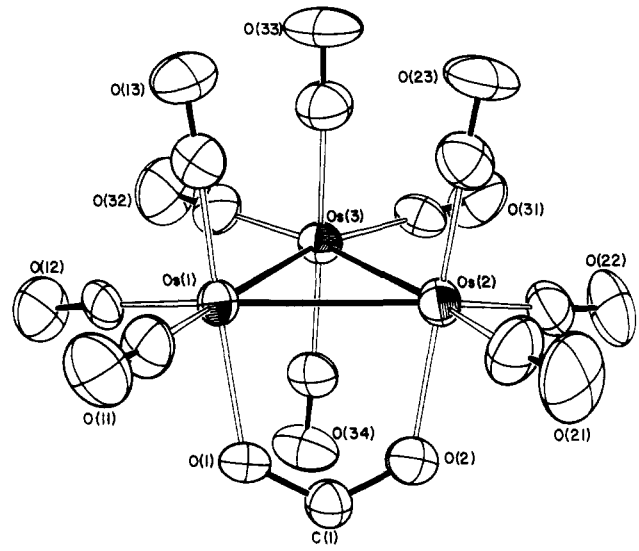

Figure 1. Molecular geometry of $(\mu\text{-H})(\mu\text{-O}_2\text{CH})\text{Os}_3(\text{CO})_{10}$. The thermal ellipsoids and geometry correspond to molecule A. The labeling scheme is valid for molecule A or B (ORTEP-II diagram).

Results and Discussion

Description of the Structure. The crystal structure consists of discrete molecules of $(\mu\text{-H})(\mu\text{-O}_2\text{CH})(\text{Os}_3(\text{CO})_{10}$, separated by normal van der Waals distances; there are no abnormally short intermolecular contacts. There are two crystallographically independent molecules ("A" and "B") in the cell forming alternate layers perpendicular to *b* in the crystal lattice.

Figure 1 shows a labeling diagram appropriate to either molecule, and Figure 2 shows a stereoscopic view of a molecule. Tables VI and VII give the interatomic distances and angles for both molecules.

Each molecule contains a triangular triosmium core in which one osmium atom (Os(3)) is linked to four terminal carbonyl ligands; the other two osmium atoms (Os(1) and Os(2)) are each linked to three terminal carbonyl ligands, are bridged diaxially by a formate moiety, and are bridged diequatorially by a hydride ligand (which was *not* located directly, but whose position can be deduced unambiguously, vide infra). Each molecule possesses approximate C_s symmetry.

A. Location of the Hydride Ligand. The μ-hydride ligands of the two independent molecules were not located directly in this study. Nevertheless, we can confidently assign their positions on the basis of the following observations.

(1) The Os(1)–Os(2) distance in each molecule is lengthened vis-à-vis the other two metal–metal distances. The average value of 2.908 Å is 0.033 Å larger than the average (2.875 [5] Å) of the nonbridged osmium–osmium distances. This latter value agrees well with the average Os–Os distance of 2.877 [3] Å found within the parent cluster $\text{Os}_3(\text{CO})_{12}$.[40]

(2) A survey of the disposition of carbonyl ligands within the equatorial triosmium plane (see Figure 3) shows a pattern of Os–Os–C and C–Os–C angles that is in all ways similar

(37) St. George, G. M. Ph.D. Thesis, University of Illinois, Urbana, IL, 1982.
(38) Graham, G. C.; Jones, W. D. *J. Mol. Spectrosc.* **1965**, *18*, 202.
(39) Mills, I. M. *Spectrochim. Acta* **1963**, *19*, 1585.
(40) Part 1: Churchill, M. R.; DeBoer, B. G. *Inorg. Chem.* **1977**, *16*, 878.

Table III. Anisotropic Thermal Parameters[a] for (μ-H)(μ-O_2CH)$Os_3(CO)_{10}$

atom	B_{11}	B_{22}	B_{23}	B_{12}	B_{13}	B_{23}
			(A) Molecule A			
Os(1A)	2.327 (26)	2.687 (24)	2.551 (26)	0.134 (19)	−0.200 (20)	−1.085 (20)
Os(2A)	3.031 (29)	2.760 (25)	2.610 (27)	−0.123 (21)	−0.190 (22)	−0.965 (21)
O(3A)	2.766 (29)	2.884 (25)	2.897 (27)	0.436 (20)	−0.492 (21)	−1.500 (21)
O(1A)	3.51 (51)	3.51 (45)	2.95 (46)	0.19 (40)	−1.08 (40)	−1.72 (38)
O(2A)	3.89 (54)	4.54 (51)	3.59 (55)	−0.22 (41)	−0.57 (44)	−2.08 (44)
C(1A)	3.0 (8)	3.8 (7)	3.1 (8)	0.1 (6)	−0.4 (6)	−1.5 (6)
O(11A)	5.8 (7)	5.9 (6)	5.0 (6)	1.1 (5)	0.0 (5)	−2.9 (5)
O(12A)	8.3 (8)	3.1 (5)	5.3 (7)	−1.6 (5)	−0.2 (6)	−1.0 (5)
O(13A)	4.2 (7)	9.8 (9)	5.8 (7)	−1.1 (6)	−1.7 (6)	−3.7 (6)
O(21A)	10.7 (10)	2.6 (5)	7.3 (8)	−0.8 (6)	0.2 (7)	−1.1 (5)
O(22A)	4.4 (7)	7.6 (7)	4.0 (6)	0.1 (6)	1.7 (5)	−1.0 (5)
O(23A)	7.0 (8)	6.7 (7)	4.2 (6)	0.8 (5)	−3.3 (6)	−2.5 (5)
O(31A)	3.4 (6)	8.2 (8)	8.1 (8)	−0.5 (5)	0.7 (6)	−5.6 (7)
O(32A)	8.7 (9)	3.5 (6)	7.3 (8)	−0.3 (6)	−1.1 (7)	−1.2 (6)
O(33A)	6.4 (8)	9.2 (8)	6.4 (8)	1.2 (6)	−4.2 (7)	−4.4 (7)
O(34A)	4.7 (6)	7.1 (7)	5.1 (6)	2.3 (5)	−2.0 (5)	−4.0 (6)
C(11A)	3.0 (8)	4.3 (8)	4.5 (9)	0.5 (6)	0.4 (6)	−2.5 (7)
C(12A)	4.0 (8)	4.0 (8)	2.8 (7)	−0.6 (6)	0.9 (6)	−2.1 (7)
C(13A)	3.5 (8)	3.9 (7)	3.9 (8)	0.8 (6)	−0.6 (7)	−1.8 (6)
C(21A)	5.4 (10)	3.4 (8)	5.9 (10)	−0.8 (7)	0.2 (8)	−2.2 (8)
C(22A)	4.3 (9)	4.7 (8)	2.9 (8)	−0.1 (7)	−0.5 (7)	−0.8 (7)
C(23A)	5.3 (10)	3.7 (8)	3.8 (8)	0.5 (7)	−1.0 (7)	−1.4 (7)
C(31A)	3.9 (8)	4.2 (8)	3.2 (7)	1.2 (6)	−0.8 (6)	−2.3 (6)
C(32A)	2.4 (7)	4.9 (9)	4.8 (9)	0.5 (7)	−0.5 (6)	−2.2 (8)
C(33A)	4.0 (9)	5.2 (9)	4.6 (9)	0.4 (7)	−1.3 (7)	−2.2 (7)
C(34A)	3.1 (8)	4.3 (8)	3.8 (8)	0.9 (6)	−0.4 (6)	−2.6 (7)
			(B) Molecule B			
Os(1B)	2.928 (28)	2.569 (24)	2.984 (27)	0.365 (20)	−0.606 (22)	−1.277 (21)
Os(2B)	2.884 (27)	2.465 (23)	2.746 (27)	0.287 (20)	−0.417 (21)	−1.288 (20)
Os(3B)	3.422 (31)	3.775 (28)	3.040 (29)	−0.202 (23)	−0.500 (23)	−1.945 (24)
O(1B)	3.27 (53)	2.96 (46)	4.50 (56)	−0.40 (41)	0.25 (43)	−0.48 (40)
O(4B)	1.88 (44)	5.14 (57)	3.64 (50)	−0.34 (39)	0.33 (37)	−2.13 (45)
C(1B)	5.5 (10)	2.5 (7)	3.6 (8)	0.3 (7)	−1.2 (7)	−1.3 (6)
O(11B)	5.2 (7)	4.5 (6)	8.0 (8)	0.4 (5)	−1.9 (6)	−3.5 (6)
O(12B)	8.5 (9)	5.3 (6)	5.1 (7)	1.7 (6)	−3.3 (7)	−1.3 (5)
O(13B)	4.3 (7)	5.6 (6)	6.0 (7)	0.1 (5)	0.3 (6)	−2.1 (5)
O(21B)	5.4 (6)	4.2 (5)	4.4 (6)	0.6 (4)	−2.8 (5)	−1.6 (4)
O(22B)	6.1 (7)	5.3 (6)	7.4 (7)	1.3 (5)	−1.0 (6)	−4.8 (6)
O(23B)	5.7 (8)	6.8 (7)	3.9 (6)	−1.6 (6)	0.7 (5)	−0.7 (5)
O(31B)	12.2 (12)	6.0 (8)	11.3 (11)	0.9 (8)	−2.5 (9)	−6.2 (8)
O(32B)	5.8 (7)	8.6 (8)	3.8 (6)	1.1 (6)	−1.8 (6)	−2.6 (6)
O(33B)	5.4 (7)	6.4 (7)	5.7 (7)	−2.1 (6)	1.3 (6)	−1.8 (6)
O(34B)	5.8 (8)	8.6 (8)	4.9 (7)	−1.5 (6)	0.5 (6)	−3.1 (6)
C(11B)	2.9 (7)	3.0 (7)	3.8 (8)	−0.4 (6)	−0.0 (6)	−1.3 (6)
C(12B)	3.3 (7)	3.3 (7)	3.8 (8)	−0.7 (6)	−0.0 (7)	−1.5 (7)
C(13B)	2.5 (7)	4.1 (8)	3.4 (8)	0.8 (6)	0.3 (6)	−1.6 (6)
C(21B)	3.3 (8)	2.6 (6)	3.1 (7)	−0.1 (5)	−0.8 (6)	−0.7 (6)
C(22B)	4.4 (9)	3.8 (7)	4.0 (8)	0.4 (7)	−0.8 (7)	−2.4 (7)
C(23B)	5.2 (10)	5.0 (9)	4.3 (9)	1.1 (8)	−2.3 (8)	−3.2 (8)
C(31B)	6.1 (11)	5.0 (9)	4.8 (9)	−1.1 (8)	−0.9 (8)	−2.3 (8)
C(32B)	5.1 (10)	4.6 (8)	1.6 (7)	−0.7 (6)	0.1 (6)	−1.2 (6)
C(33B)	3.8 (8)	4.4 (8)	3.3 (8)	0.2 (7)	−1.1 (7)	−1.8 (7)
C(34B)	4.1 (9)	6.5 (10)	3.0 (8)	−2.3 (7)	1.9 (7)	−3.3 (7)

[a] The anisotropic thermal parameters are in the form $\exp[-0.25(h^2a^{*2}B_{11} + k^2b^{*2}B_{22} + l^2c^{*2}B_{33} + 2hka^*b^*B_{12} + 2hla^*c^*B_{13} + 2klb^*c^*B_{23})]$.

Table IV. Symmetry Coordinates for the Formate Ligand

S_1: r_{CH}
S_2: $(1/2^{1/2})(r_{CO_a} + r_{CO_b})$
S_3: $r_{CO}(\angle OCO)$
S_4: $(1/2^{1/2})(r_{CO_a} - r_{CO_b})$
S_5: $^1/_2 r_{CH}(\angle HCO_a - \angle HCO_b)$
S_6: $r_{CH}\gamma$[a]

[a] γ = out-of-plane angle.

Table V. Calculated Force Constants for the Formate Ligand (mdyn/A)

Diagonal Force Constants	
$F_{11} = 4.780$	$F_{44} = 7.718$
$F_{22} = 13.754$	$F_{55} = 1.052$
$F_{33} = 1.303$	$F_{66} = 0.346$
Interaction Constants	
$F_{12} = -0.237$	$F_{23} = 1.652$
$F_{13} = -0.160$	$F_{45} = 0.628$

to the pattern seen in other triangular clusters containing μ-hydride ligands within the equatorial plane (viz., (μ-H)(H)$Os_3(CO)_{11}$[40] and (μ-H)(H)$Os_3(CO)_{10}(PPh_3)$[41] and triangular clusters in general).[42] Thus, the equatorial Os–Os–C angles adjacent to the Os(1)–Os(2) bond average 117 [2]° (as compared to 93.2° in $Os_3(CO)_{12}$)[40] and the subsequent C–Os–C angles are reduced substantially from the average value of 103.5° in $Os_3(CO)_{12}$.

These effects are consistent with a μ-hydride ligand (in a diequatorial site) bridging the Os(1)–Os(2) bond. We can,

(41) Part 3: Churchill, M. R.; DeBoer, B. G. *Inorg. Chem.* **1977**, *16*, 2897.
(42) Churchill, M. R. *Adv. Chem. Ser.* **1978**, *No. 167*, 36.

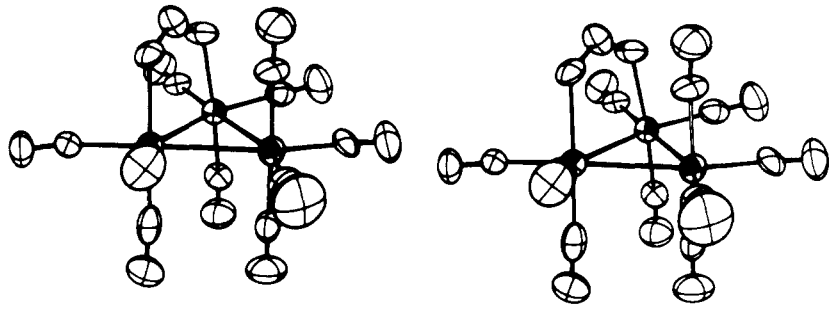

Figure 2. Stereoscopic view of molecule A.

Table VI. Interatomic Distances (Å) for $(\mu\text{-H})(\mu\text{-O}_2\text{CH})\text{Os}_3(\text{CO})_{10}$

atoms	dist molecule A	dist molecule B
(A) Osmium-Osmium Distances		
Os(1)-Os(2)	2.9158 (10)	2.9013 (9)
Os(1)-Os(3)	2.8701 (9)	2.8774 (8)
Os(2)-Os(3)	2.8728 (9)	2.8811 (9)
av Os-Os (bridged) 2.909 [10]		
av Os-Os (nonbridged) 2.875 [5]		
(B) Osmium-Carbonyl Distances		
Os(1)-C(11)	1.933 (14)	1.952 (14)
Os(1)-C(12)	1.930 (15)	1.902 (16)
Os(1)-C(13)	1.888 (16)	1.872 (15)
Os(2)-C(21)	1.929 (15)	1.964 (14)
Os(2)-C(22)	1.961 (16)	1.881 (14)
Os(2)-C(23)	1.916 (16)	1.902 (18)
Os(3)-C(31)	1.914 (15)	1.942 (17)
Os(3)-C(32)	1.960 (16)	1.947 (16)
Os(3)-C(33)	1.992 (16)	1.966 (16)
Os(3)-C(34)	1.949 (15)	1.974 (16)
av Os-CO (all) 1.934		
av Os-CO (CO trans) 1.970 [18]		
av Os-CO (O trans) 1.895 [19]		
av Os-CO (eq) 1.935 [25]		
(C) Osmium-Oxygen Distances		
Os(1)-O(1)	2.160 (8)	2.152 (19)
Os(2)-O(2)	2.158 (9)	2.175 (9)
(D) Distances within Formate Ligands		
C(1)-O(1)	1.245 (15)	1.238 (16)
C(1)-O(2)	1.249 (16)	1.271 (15)
O(1)···O(2)	2.229 (14)	2.263 (13)
av C-O 1.251 [14]		
(E) C-O (Carbonyl) Distances		
C(11)-O(11)	1.136 (15)	1.119 (14)
C(12)-O(12)	1.118 (16)	1.147 (16)
C(13) O(13)	1.106 (16)	1.113 (16)
C(21)-O(21)	1.115 (16)	1.111 (14)
C(22)-O(22)	1.091 (17)	1.127 (15)
C(23)-O(23)	1.111 (16)	1.120 (18)
C(31)-O(31)	1.135 (16)	1.128 (18)
C(32)-O(32)	1.104 (16)	1.117 (16)
C(33)-O(33)	1.088 (16)	1.133 (16)
C(34)-O(34)	1.134 (15)	1.094 (16)

in fact, further specify the site of the hydride ligand. The carbonyl ligands C(12)–O(12) and C(22)–O(22) lie trans to the bridging hydride ligand. Since they are displaced slightly from the triosmium plane (*toward* the formate group), it follows that the hydride ligand is also displaced slightly from the triosmium plane, in a direction *away* from the formate group. The average displacement of −0.39 Å for the trans carbon, taken in conjunction with the (equatorial) Os–CO bond length of 1.94 Å in the present complex and the known Os–$(\mu$-H) distance of ~1.85 Å,[43] suggests that the hydride ligand suffers a proportional displacement of about +0.37 Å from the triosmium plane. This value is, however, a "guesstimate".

(43) For neutron diffraction studies of $(\mu\text{-H})_2\text{Os}_3(\text{CO})_{10}$ see ref 13 and 14.

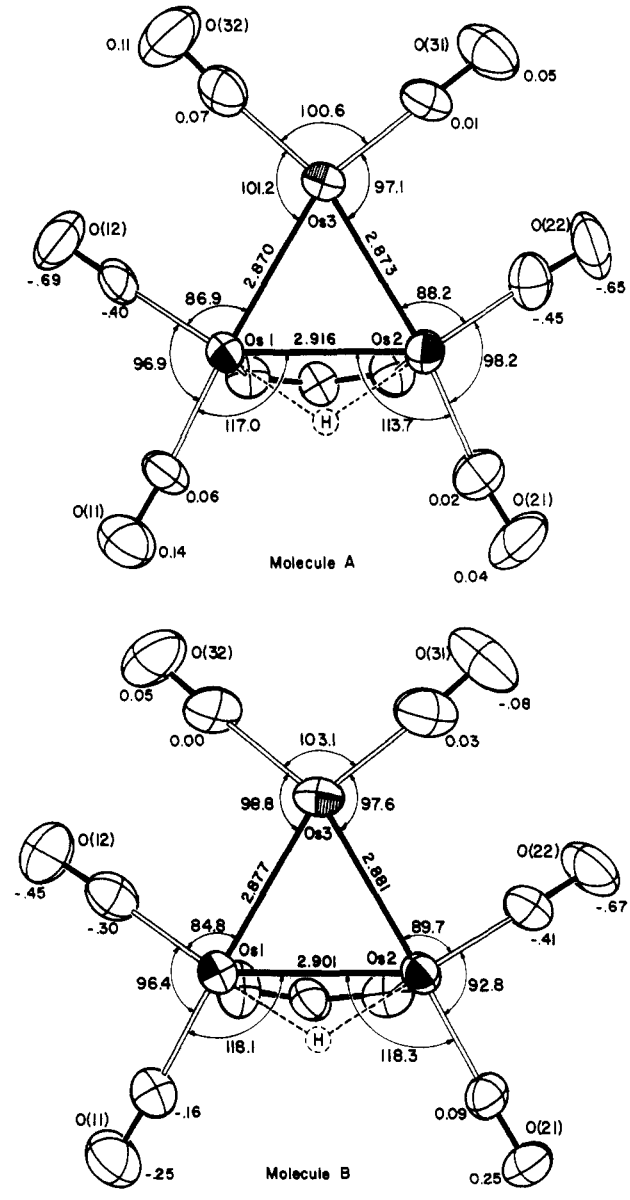

Figure 3. Distances and angles within the equatorial plane for molecules A and B. The bridging hydride ligand is shown in its deduced position. Small numbers appear near the oxygen and carbon atoms give the deviation (in Å) of that atom from the triosmium plane.

B. Formate Ligand. The bridging formate ligand has the expected geometry with an average O–C–O angle of 127.8° and equivalent C–O bond distances averaging 1.251 [14] Å—i.e., in the normal range for delocalized carboxylic acid anions.

Table VII. Interatomic Angles (Deg) for (μ-H)(μ-O_2CH)$Os_3(CO)_{10}$

atoms	angle, molecule A	angle, molecule B
(A) Os-Os-Os Angles		
Os(2)-Os(1)-Os(3)	59.53 (2)	59.81 (2)
Os(1)-Os(2)-Os(3)	59.44 (2)	59.68 (2)
Os(1)-Os(3)-Os(2)	61.02 (2)	60.51 (2)
(B) Equatorial Os-Os-C and C-Os-C Angles		
Os(2)-Os(1)-C(11)	117.0 (4)	118.1 (4)
Os(3)-Os(1)-C(12)	86.9 (4)	84.8 (4)
C(11)-Os(1)-C(12)	96.9 (6)	96.4 (6)
Os(1)-Os(2)-C(21)	113.7 (5)	118.3 (4)
Os(3)-Os(2)-C(22)	88.2 (4)	89.7 (4)
C(21)-Os(2)-C(22)	98.7 (7)	92.8 (6)
Os(1)-Os(3)-C(32)	101.2 (4)	98.8 (4)
Os(2)-Os(3)-C(31)	97.1 (4)	97.6 (5)
C(31)-Os(3)-C(32)	100.6 (6)	103.1 (6)
(C) Angles Involving Axial Ligands		
O(1)-Os(1)-Os(2)	80.5 (2)	81.5 (2)
O(1)-Os(1)-Os(3)	93.9 (2)	91.6 (3)
O(1)-Os(1)-C(11)	87.0 (5)	83.5 (5)
O(1)-Os(1)-C(12)	91.6 (5)	91.8 (5)
C(13)-Os(1)-Os(2)	97.6 (5)	98.2 (4)
C(13)-Os(1)-Os(3)	87.4 (4)	92.1 (4)
C(13)-Os(1)-C(11)	91.5 (6)	92.8 (6)
C(13)-Os(1)-C(12)	91.5 (6)	91.0 (6)
C(13)-Os(1)-O(1)	176.7 (5)	175.6 (6)
O(2)-Os(2)-Os(1)	81.2 (3)	81.5 (2)
O(2)-Os(2)-Os(3)	92.8 (2)	93.0 (2)
O(2)-Os(2)-C(21)	86.2 (6)	89.0 (5)
O(2)-Os(2)-C(22)	88.8 (5)	89.0 (5)
C(23)-Os(2)-Os(1)	98.6 (5)	99.7 (4)
C(23)-Os(2)-Os(3)	90.8 (4)	88.8 (4)
C(23)-Os(2)-C(21)	89.9 (7)	89.1 (6)
C(23)-Os(2)-C(22)	93.8 (7)	90.8 (6)
C(23)-Os(2)-O(2)	175.6 (6)	178.2 (6)
C(33)-Os(3)-Os(1)	90.9 (5)	89.6 (4)
C(33)-Os(3)-Os(2)	90.1 (4)	90.0 (4)
C(33)-Os(3)-C(31)	88.8 (6)	89.7 (7)
C(33)-Os(3)-C(32)	88.1 (6)	89.8 (6)
C(34)-Os(3)-Os(1)	85.4 (4)	87.7 (4)
C(34)-Os(3)-Os(2)	88.1 (4)	86.8 (5)
C(34)-Os(3)-C(31)	94.7 (6)	92.1 (7)
C(34)-Os(3) C(32)	92.6 (6)	92.6 (7)
C(34)-Os(3)-C(33)	176.3 (7)	176.6 (6)
(D) Angles within Formate Ligands		
Os(1)-O(1)-C(1)	126.1 (9)	124.8 (9)
Os(2)-O(2)-C(1)	125.2 (9)	123.0 (10)
O(1)-C(1)-C(2)	126.7 (13)	128.9 (15)
(E) Os-C-O Angles		
Os(1)-C(11)-O(11)	176.2 (18)	177.0 (20)
Os(1)-C(12)-O(12)	176.7 (21)	177.1 (22)
Os(1)-C(13)-O(13)	176.6 (20)	175.3 (14)
Os(2)-C(21)-O(21)	172.3 (18)	174.1 (14)
Os(2)-C(22)-O(22)	176.1 (18)	179.1 (9)
Os(2)-C(23)-O(23)	177.6 (11)	176.3 (18)
Os(3)-C(31)-O(31)	178.4 (10)	172.6 (19)
Os(3)-C(32)-O(32)	176.4 (20)	176.6 (20)
Os(3)-C(33)-O(33)	174.2 (18)	176.3 (17)
Os(3)-C(34)-O(34)	176.2 (16)	175.0 (18)

The overall orientation of the formate ligand may be described in terms of two dihedral angles—the sequential angles between the Os_3 plane, the O(1)–Os(1)–Os(2)–O(2) plane, and the O(1)–C(1)–O(2) plane. These least-squares planes, and atomic deviations therefrom, are compiled in Table VIII.

In molecule A, the Os_3 plane makes an angle of 99.5° with the O(1)–Os(1)–Os(2)–O(2) "coordination plane"; the formate ligand (defined by O(1)–C(1)–O(2)) bends outward by a further 5.6° from this coordination plane. Analogous angles for molecule B are 97.7 and 4.9°, respectively. The further bending of the formate ligand from the "coordination plane" probably results from intramolecular repulsion between the

Table VIII. Least-Squares Planes in (μ-H)(μ-O_2CH)$Os_3(CO)_{10}$

(a) Triosmium Planes[a]

	A	B	C	D
molecule A	−0.7089	−0.2729	−0.6503	−4.3747
molecule B	−0.6782	−0.2228	0.7003	1.5092

atom	dist to plane, A, molecule A	dist to plane, A, molecule B
Os(1)[b]	0.0	0.0
Os(2)[b]	0.0	0.0
Os(3)[b]	0.0	0.0
C(11)	0.059 (16)	−0.159 (15)
O(11)	0.139 (12)	−0.258 (13)
C(12)	−0.401 (16)	−0.299 (16)
O(12)	−0.691 (12)	−0.448 (13)
C(21)	0.016 (18)	0.088 (15)
O(21)	0.041 (14)	0.245 (11)
C(22)	−0.451 (17)	−0.414 (16)
O(22)	−0.652 (13)	−0.674 (12)
C(31)	0.009 (16)	0.028 (19)
O(31)	0.046 (13)	−0.075 (16)
C(32)	0.071 (17)	−0.001 (16)
O(32)	0.113 (14)	0.054 (13)

(b) "Coordination Planes"–O-Os-Os-O

	A	B	C	D
molecule A	−0.5262	0.8496	−0.0354	1.3496
molecule B	0.3453	0.6042	0.7182	8.8843

atom	dist to plane, A, molecule A	dist to plane, A, molecule B
Os(1)[b]	−0.0152 (6)	0.0166 (6)
Os(2)[b]	0.0152 (6)	−0.0163 (6)
O(1)[b]	0.020 (10)	−0.021 (10)
O(2)[b]	−0.020 (10)	0.021 (10)
C(1)	0.054 (15)	0.045 (16)
C(13)	0.045 (16)	0.192 (15)
O(13)	0.135 (13)	0.365 (12)
C(23)	0.193 (17)	−0.002 (18)
O(23)	0.339 (12)	0.065 (13)
Os(2)	−2.440 (1)	−2.464 (1)

(c) "Formate" Planes

	A	B	C	D
molecule A	−0.5739	0.8113	−0.1114	0.6828
molecule B	0.2725	0.5895	0.7604	8.8138

atom	dist to plane, A, molecule	dist to plane, A, molecule B
O(1)[b]	0.0	0.0
O(2)[b]	0.0	0.0
C(1)[b]	0.0	0.0
Os(1)	0.1627 (6)	0.2208 (6)
Os(2)	0.2450 (6)	0.1366 (6)
Os(3)	−2.1853 (6)	−2.2484 (6)

Angles between Planes (Deg)

	molecule A	molecule B
a/b	99.5	99.7
b/c	5.6	4.9
a/c	104.9	102.5

[a] A, B, C, and D are the coefficients for the equation of the plane $AX + BY + CZ = D$, where X, Y, and Z are the orthonormal-coordinate system based on $B \times C^*$, B, and C^*. The conversion matrix is

$$\begin{pmatrix} X \\ Y \\ Z \end{pmatrix} = \begin{pmatrix} 7.9643 & 0 & 2.5039 \\ 0.2525 & 15.316 & 6.4453 \\ 0 & 0 & 14.144 \end{pmatrix} \begin{pmatrix} x \\ y \\ z \end{pmatrix}$$

[b] Atoms used in calculation of plane.

Table IX. Selected Intramolecular Contacts (Å)

	A	B
C(1)-C(34)	2.868 (17)	2.863 (20)
C(1)-O(34)	2.926 (19)	2.840 (18)
O(1)-C(34)	2.911 (16)	3.043 (15)
O(2)-C(34)	2.934 (16)	3.095 (15)

formate ligand and carbonyl group C(33)–O(33) (see Table IX).

The short "bite" of the formate ligand (O(1)···O(2) average 2.246 Å) relative to the bridged Os(1)–Os(2) distance (average 2.908 Å) results in the angles Os(1)–Os(2)–O(2) and Os(2)–Os(1)–O(1) being acute (average 81.2 [5]°). This, in turn, leads to obtuse Os–Os–CO angles for those carbonyl ligands trans to the formate group (the average of the Os(1)–Os(2)–C(23) and Os(2)–Os(1)–C(13) angles is 98.5 [9]°). This distortion of the axial ligands (relative to their location in $Os_3(CO)_{12}$) is accompanied by displacement of the carbonyl groups C(12)–O(12) and C(22)–O(22) toward the formate side of the triosmium plane (vide supra).

Thus, as with $Os_3(CO)_{12}$, the environments of Os(1) and Os(2) approximate to octahedral; the axes of these octahedra in the present complex are tipped, relative to those in $Os_3(CO)_{12}$, via equivalent (disrotatory) rotations about the O(11)···Os(1)–Os(3) and O(21)···Os(2)–Os(3) axes.

C. Effect of the Diaxially Bridging Formate Ligand upon the Equatorially μ-Hydrido-Bridged Os(1)–Os(2) Distances. Previous work[42] has shown that an unsupported equatorially bridging hydride ligand causes an increase in the bridged metal–metal bond of ~0.15 Å over the normal M–M σ-bond length. In the present complex the increase is restricted to about 0.033 Å because it is *opposed* by the small bite of the diaxially bridging formate ligand.

A similar effect is found in the triosmium fragment of the [(μ-H)$Os_9(CO)_{27}(CO_2)^-$] anion[20] (see III), where the μ-hydrido-bridged Os–Os distance (which is also bridged by a $-CO_2^-$ moiety) is 2.895 (7) Å as compared to 2.870 Å for the other two bonds. In keeping with this, the bis(acetato)-bridged osmium–osmium distance in the dinuclear complex (μ-$O_2CMe)_2Os_2(CO)_6$ is reduced to 2.730 (2) and 2.732 (2) Å in the two independent molecules.[44]

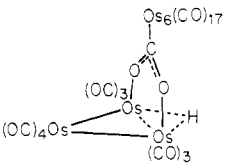

III

The effect also is seen for the dithioformate complex (μ-H)(μ-$S_2CH)Os_3(CO)_{10}$,[22a] where in two independent molecules the doubly bridged Os–Os distances (2.978 (1) and 2.968 (1) Å) average 0.065 Å longer than the unbridged distances. When the osmium–osmium vector is bridged only by the dithioformate ligand, as in (μ-H)(μ-$S_2CH)Os_3(CO)_9(P(CH_3)_2C_6H_5)$,[22] the Os–Os distance relaxes to 2.854 (1) Å.

Vibrational Modes of the Formate Ligand. The infrared bands due to the formate ligand in (μ-H)(μ-$O_2CH)Os_3(CO)_{10}$, (μ-H)(μ-$O_2CD)Os_3(CO)_{10}$, and (μ-H)(μ-$O_2{}^{13}CH)Os_3(CO)_{10}$ were assigned by observation of frequency changes due to isotopic substitution and by comparison with spectra reported for other formate compounds.[45,46] The assignments were confirmed by satisfactory agreement between the observed frequencies and calculated frequencies on the basis of a simplified normal-coordinate analysis of the vibrationally isolated formate group. The observed and calculated frequencies together with their assignments are listed in Table X. The spectrum of (μ-H)(μ-$O_2CD)Os_3(CO)_{10}$ in a KBr pellet is shown in Figure 4. The in-plane C–H (C–D) bend was observed unambiguously for (μ-H)(μ-$O_2CD)Os_3(CO)_{10}$. In the undeuterated compounds, however, this band was generally difficult to distinguish from the strong symmetric C–O stretch ($\nu^s_{CO_2}$). In the KBr-pellet spectrum of (μ-H)(μ-$O_2{}^{12}CH)Os_3(CO)_{10}$ a weak band at 1370 cm^{-1} was apparent on the side of the strong $\nu^s_{CO_2}$ band; this is reported as δ_{CH} in Table X but was not included in the force constant refinement. In the spectrum of (μ-H)(μ-$O_2{}^{13}CH)Os_3(CO)_{10}$ the corresponding band was obscured by $\nu^s_{CO_2}$ of the unlabeled compound present (ca. 10%) in the sample.

Table X. Calculated and Observed Formate Vibrational Frequencies (cm^{-1})

	(μ-H)(μ-$O_2{}^{12}CH)Os_3(CO)_{10}$		(μ-H)(μ-$O_2CD)Os_3(CO)_{10}$		(μ-H)(μ-$O_2{}^{13}CH)Os_3(CO)_{10}$	
mode	calcd	obsd	calcd	obsd	calcd	obsd
ν_{CH}	2972	2978	2207	2210	2962	2960
$\nu^s_{CO_2}$	1359	1362	1332	1338	1348	1338
δ_{OCO}	798	794	784	784	785	786
$\nu^a_{CO_2}$	1576	1576	1571	1572	1534	1533
δ_{CH}	1376	1370[a]	1008	1009	1376	[b]
π_{CH}	1032	1031	879	887	1016	1016

[a] This band was observed only in the KBr pellet spectrum; its position was not included in the force constant refinement. [b] This band was obscured by the presence of (μ-H)(μ-$O_2{}^{13}CH)Os_3(CO)_{10}$ (ca. 10%) in the sample.

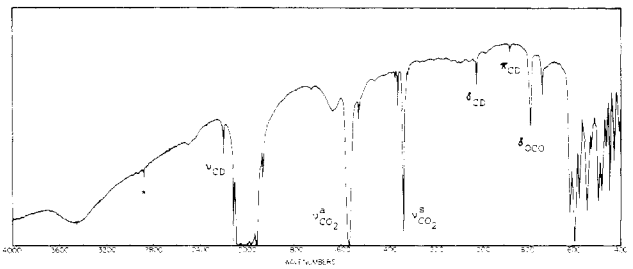

Figure 4. Infrared spectrum of (μ-H)(μ-$O_2CD)Os_3(CO)_{10}$ dispersed in KBr. The asterisk marks the position (2896 cm^{-1}) of a relatively intense combination band (see text).

The assignments of ν_{CH} in Table X are dependent on the assignment of ν_{CD} (see Figure 4). Two bands of nearly equal intensity at 2978 and 2899 cm^{-1} were observed for (μ-H)(μ-$O_2CH)Os_3(CO)_{10}$. A third band at ca. 2925 cm^{-1} was seen in solution spectra, but it was broad and weak, and both its position and intensity changed in the KBr spectrum. The highest frequency band disappeared in the spectrum of the deuterated compound; hence, it has been assigned to ν_{CH} for (μ-H)(μ-$O_2CH)Os_3(CO)_{10}$. The remaining bands are presumably combination bands. A band of intensity comparable to ν_{CH} in the spectrum of aqueous potassium formate was assigned as a combination of the antisymmetric modes $\nu^a_{CO_2}$ and δ_{CH}.[45] This assignment is not satisfactory in the present case, since the strong band is in essentially the same position (2896 cm^{-1}) for (μ-H)(μ-$O_2CD)Os_3(CO)_{10}$. The band must involve the formate ligand, since it shifts markedly (to 2876 cm^{-1}) in the spectrum of (μ-H)(μ-$O_2{}^{13}CH)Os_3(CO)_{10}$. Perhaps the most likely explanation is a combination of δ_{OCO} and a symmetric metal carbonyl stretching mode; e.g., for (μ-H)(μ-$O_2CH)Os_3(CO)_{10}$, 2115 + 794 = 2909, which is very close to the observed value. The combination band may gain intensity at the expense of ν_{CH} through Fermi resonance. Indeed, ν_{CD} appeared to be significantly more (ca. 2.7) intense than ν_{CH} and the corresponding combination band less intense, as would be expected for the much greater frequency sepa-

(44) Bullitt, J. G.; Cotton, F. A. *Inorg. Chim. Acta* **1971**, *5*, 406.
(45) Ito, K.; Bernstein, H. J. *Can. J. Chem.* **1956**, *34*, 170.
(46) Dixon, R. N. *J. Chem. Phys.* **1959**, *31*, 258.

Table XI. Vibrational Frequency (cm^{-1}) Comparison with Formate on a Silver Surface (300 K)[a]

mode	HCO_2/ Ag(110)	(μ-H)-(μ-O_2CH)-$Os_3(CO)_{10}$	DCO_2/ Ag(110)	(μ-H)-(μ-O_2CD)-$Os_3(CO)_{10}$
ν_{CH} (ν_{CD})	2870 (w)	2978 (w)	2150 (w)	2210 (w)
$\nu^a_{CO_2}$	1570 (w)	1576 (vs)	1570 (w)	1572 (vs)
δ_{CH} (δ_{CD})		1370 (w)	1020 (w)	1009 (w)
$\nu^s_{CO_2}$	1340 (s)	1362 (s)	1300 (s)	1338 (s)
π_{CH} (π_{CD})	1060 (w)	1031 (vw)		887 (vw)
δ_{OCO}	760 (m)	794 (m)	750 (m)	784 (m)

[a] Abbreviations: s, strong; m, medium; w, weak; vw, very weak.

ration in the deuterated compound. A resonance interaction would also shift the position of ν_{CH} to higher energy and of the combination band to lower energy, but the calculated[37,46] magnitude of the shift is only about 3 cm^{-1}.

The C–H stretching frequency found for (μ-H)(μ-O_2CH)$Os_3(CO)_{10}$ is markedly higher than for most other formate complexes,[47,48] including those in which the formate ligand is bridging (e.g. $Rh_2(\mu\text{-}O_2CH)_4(OH_2)_2$, 2870, 2840 cm^{-1};[49] $Mo_2(\mu\text{-}O_2CH)_4$, 2970, 2820 cm^{-1} [50]). This is not a structural effect due to opening of the O–C–O angle, since computer analysis shows that ν_{CH} decreases monotonically as this angle increases. Several studies have compared ν_{CH} in alkali, alkaline-earth, and rare-earth formates with the relative covalent character in the metal–formate band, as deduced from electronegativity arguments, and concluded that ν_{CH} increases with increasing covalency.[48,51] Ab initio molecular orbital calculations[52] have suggested that covalent interaction between the formate ion and a cation results in extensive charge transfer from the oxygen atoms, which in turn makes the carbon atom significantly more electronegative. Spectroscopically, these changes in charge distribution should lead to an increase in the force constant and hence the frequency of the C–H stretch. A relatively more electronegative charge atom also should lead to a relatively higher value of the ^{13}C–^1H coupling constant.[53] The value of $^1J_{CH}$ in (μ-H)(μ-$O_2{}^{13}$CH)$Os_3(CO)_{10}$ is 219 Hz, which is much closer to the value for methyl formate (226 Hz)[54] than that for sodium formate (195 Hz).[54] Thus, both $^1J_{CH}$ and ν_{CH} indicate high covalency in the formate–osmium cluster bond. Charge transfer very likely is facilitated by the π-acceptor character of the carbonyl ligands.

Comparison with Formate Chemisorbed on a Metal Surface. Studies of chemisorbed formate by infrared spectroscopy in general have not provided all six frequencies, due to the inherently low intensity of some of the bands or to overlap with bands of an oxide support. However, the recent work of Sexton[7] and Sexton and Madix,[8] in which electron energy loss spectroscopy (EELS) was utilized to examine formic acid adsorbed on Cu(100) and Ag(110) single-crystal surfaces, has provided a complete set of formate frequencies. In the silver case deuterated formic acid was examined also, so that data for both $-O_2CH$ and $-O_2CD$ on Ag(110) are available. These data (at 300 K) are summarized in Table XI together with the analogous data for the corresponding triosmium complexes. Good overall agreement of the vibrational frequencies of the formate group in both environments is apparent.

The dipole selection rule for EELS predicts that only vibrational modes that have dipole moment changes with components normal to the metal surface will be observable at the specular angle.[55] On this basis Sexton[7] has summarized the observable modes expected for a symmetrical chemisorbed formate moiety: (i) only ν_{CH}, $\nu^s_{CO_2}$, and δ_{OCO}, if the plane containing the formate group is perpendicular to the surface (site symmetry C_{2v}); (ii) the same three modes and π_{CH} in addition, if the formate plane is not perpendicular (site symmetry C_s). The strong attenuation of the antisymmetric modes $\nu^a_{CO_2}$ and δ_{CH} in the EELS spectrum of formate on silver at 300 K was taken to indicate that the dipole moment changes for these vibrations are nearly parallel to the surface, i.e., that the two M–O and the two C–O bonds are each equivalent under these conditions. The appearance in the spectrum of a band assigned to the inherently weak π_{CH} mode also led the authors to suggest that the formate ligand plane is tipped significantly away from the normal to the surface. Such detailed structural deductions, however, also require EELS spectra taken at off-specular angles, which was not done in these studies. The formate group presumably bridges two metal atoms on the surface. The distance between the metal centers does not appear to be a significant restriction, since a formate ligand can bridge M–M distances from 2.09 Å in $Mo_2(\mu\text{-}O_2CH)_4$[50] to 2.91 Å in (μ-H)(μ-O_2CH)$Os_3(CO)_{10}$ as reported here.

The values of ν_{CH} observed for formate on Ag(110) (2870 cm^{-1}) and Cu(100) (2910 cm^{-1}) indicate moderate covalency in the formate–surface interaction. This may depend, naturally, on the electronegativity of the metal. In a recent ultraviolet photoelectron study of formic acid decomposition on W(100),[56] a decrease in the work function upon adsorption was observed, which was taken to indicate significant charge transfer from formate to the tungsten surface. An EELS study of this system would be enlightening.

Acknowledgment. This research was supported at the University of Illinois by National Science Foundation Grants DMR 80-20250 and CHE 81-00140 and by a Camille and Henry Dreyfus Teacher-Scholar Grant (to J.R.S.). The work at SUNY—Buffalo was supported by National Science Foundation Grant CHE 80-23448 (to M.R.C.). The Nicolet 7199C FT IR spectrometer used in this work at the University of Illinois was purchased in part by funds from an instrumentation grant, NSF CHE 80-17761.

Registry No. (μ-H)(μ-O_2CH)$Os_3(CO)_{10}$, 64443-52-3; $Os_3(CO)_{10}(C_8H_{14})_2$, 61840-78-6.

Supplementary Material Available: A listing of observed and calculated structure factor amplitudes (27 pages). Ordering information is given on any current masthead page.

(47) Donaldson, J. D.; Knifton, J. F.; Ross, S. D. *Spectrochim. Acta* **1964**, *20*, 847.
(48) Kartha, V. B.; Sugandhi, J. S. *Indian J. Phys.* **1976**, *50*, 115.
(49) Shafranskii, V. N.; Nalkova, T. A. *Zh. Obshch. Khim.* **1976**, *46*, 1197.
(50) Cotton, F. A.; Norman, J. G.; Stultz, B. R.; Webb, T. R. *J. Coord. Chem.* **1975**, *5*, 217.
(51) Nefedov, V. I.; Grigorev, A. I.; Turova, N. Y.; Salyn, Y. V. *Dokl. Akad. Nauk SSSR* **1973**, *208*, 1107.
(52) Peyerimhoff, S. D.; Buenker, R. J. *J. Chem. Phys.* **1969**, *50*, 1846.
(53) Grant, D. M.; Litchman, W. M. *J. Am. Chem. Soc.* **1965**, *87*, 3994.
(54) Hammaker, R. M. *J. Mol. Spectrosc.* **1965**, *15*, 506.
(55) Ibach, H.; Hopster, H.; Sexton, B. A. *App. Surf. Sci.* **1977**, *1*, 1.
(56) Bhattacharya, A. L. *J. Chem. Soc., Faraday Trans. 1* **1979**, *75*, 863.